Modification of existing methods of visualization of offset face skin structure

Romanyuk, Sergey, Romanyuk, Olexander, Pavlov, Sergey, Romanyuk, Oksana, Dobrovolska, Nataliia, et al.

Sergey O. Romanyuk, Olexander N. Romanyuk, Sergey V. Pavlov, Oksana V. Romanyuk, Nataliia V. Dobrovolska, Liubov M. Kravchenko, Sergii V. Tymchyk, Andrzej Smolarz, Olena Kulakova, Aliya Kalizhanova, Zhazira Amirgaliyeva, "Modification of existing methods of visualization of offset face skin structure," Proc. SPIE 11456, Optical Fibers and Their Applications 2020, 114560E (12 June 2020); doi: 10.1117/12.2569770

SPIE.

Event: Optical Fibers and Their Applications 2020, 2020, Bialowieza, Poland

Modification of existing methods of visualization of offset face skin structure

Sergey O. Romanyuk[a], Olexander N. Romanyuk[a], Sergey V. Pavlov[a], Oksana V. Romanyuk[a], Nataliia V. Dobrovolska[b], Liubov M. Kravchenko[c], Sergii V. Tymchyk[a], Andrzej Smolarz[d], Olena Kulakova[e], Aliya Kalizhanova[f,g], Zhazira Amirgaliyeva[f,h]
[a]Vinnytsia National Technical University, Khmelnytsky Hwy, 95, 21021 Vinnitsa, Ukraine; [b]Vinnytsia Institute of Trade and Economics of Kyiv National University of Trade and Economics; [c]Poltava V.G. Korolenko National Pedagogical University; [d]Lublin University of Technology, Lublin, Poland; [e]Kazakh National Research Technical University named after K.I.Satpayev, Almaty, Kazakhstan; [f]Institute of Information and Computational Technologies CS MES RK, Almaty, Kazakhstan; [g]University of Power Engineering and Telecommunications, Almaty, Kazakhstan; [h]Al- Farabi Kazakh National University, Almaty, Kazakhstan

ABSTRACT

New modifications of the Cook-Torrance and Ward models are proposed, which differ from the known uses when calculating only one function and smaller degrees of polynomials, which makes it possible to improve the performance of three-dimensional image formation taking into account the offset properties of surfaces.

Keywords: Bidirectional reflectance distribution function, Cook–Torrance model, Ward model, rendering

1. INTRODUCTION

Spatial imaging [1–8] is a complex computational process. This is due to the multi-step and complexity of geometric transformations, the use of complex models of lighting and over-painting [7–12]. The final rendering (rendering) stage [1, 3, 5,7] is one of the most time consuming, as each intensity point determines the color intensity and the screen coordinates. It is important not only to accurately reproduce the shape of the object and its design features but also to correctly convey the gradation of colors since this is crucial in creating the illusion of three-dimensional volume on a two-dimensional flat screen.

In determining the intensity of the coil color of the pixels, the location of the light source and the observer, the optical properties of the material, the spectral characteristics of the light source, and the curvature of the surface are taken into account. In this regard, the final visualization is characterized by significant computational costs, which necessitates the development of methods and tools to improve the productivity of its implementation.

At the present stage of development of three-dimensional graphics, the question of dynamic graphic images formation in real-time and in interactive mode is urgently raised, when it is assumed that the trajectories of motion of objects are not predetermined but determined by the actions of the user in the process of interaction with the system. Visualization of three-dimensional scenes for such modes imposes strict requirements on methods and means of forming three-dimensional graphic scenes, which creates the task of increasing their productivity. Today, the growth rate of the geometric complexity of 3D images exceeds the growth rate of graphics performance. Insufficient graphics performance is also a hindrance to modeling in physical process scenes and increasing the number of dynamic objects.

Since the final visualization stage is the most time-consuming stage of 3D modeling and accounts for 60–80% [3] of the total amount of calculations, it is advisable to develop methods and models that would improve the performance and achieve the desired dynamics of realistic images.

*e-mail: rom8591@gmail.com

Optical Fibers and Their Applications 2020, edited by Ryszard S. Romaniuk, Jan Dorosz, Proc. of SPIE Vol. 11456, 114560E · © 2020 SPIE
CCC code: 0277-786X/20/$21 · doi: 10.1117/12.2569770

2. MODEL ANALYSIS

Testing with subsequent illumination is most often used in the formation of images of a person's face for surgical interventions. In this case, the surface area of the image obtained from patients' photographs is used as texture. This approach best conveys the relief character of the skin, its specific micro-features[1]. The surfaces of virtually all materials have the property of anisotropy, that is, the reflectivity of the material depends on the angle of view of the object by the observer relative to the normal to the surface. As the skin belongs to rough surfaces, it is often advisable to use lighting models that take into account the offset structure of the surface and, as a consequence, are more physically correct. Such models include the Cook-Torrance model[13] and the Ward model[14]. It was found [2] that the Cook-Torrance model better models the spectral component of color, and the Ward model diffuses. In these models, the surface roughness distribution is used to account for surface roughness.

3. METHOD MODIFICATION

Consider the Cook-Torrance model [13], the bend with which the calculation of reflected light is carried out by the formula

$$\frac{F \cdot G \cdot D}{(\vec{V} \cdot \vec{N}) \cdot (\vec{L} \cdot \vec{N})},$$

where F is the Fresnel coefficient of G – an option that allows self-shading fields, D is a parameter that determines the RMS slope of the microfacets.

Microfacets have the greatest impact if they are directed along the vector $\vec{H}$. Parameter D is determined by the following formula:

$$D = \frac{1}{4 \cdot m^2 (\vec{H} \cdot \vec{N})^4} e^{\left(\frac{(\vec{H} \cdot \vec{N})^2 - 1}{m^2 \cdot (\vec{H} \cdot \vec{N})^2}\right)}.$$

where m - an average slope of the microfacets. The m is selected in the range from 0.2 to 0.6.

Calculation of D is difficult as it involves the use of two functions - exponential and cosine. We will express D through one function that will simplify the computational process.

Write parameter that determines the degree exponent in the formula for calculating D in this form

$$\frac{(\vec{H} \cdot \vec{N})^2 - 1}{m^2 \cdot (\vec{H} \cdot \vec{N})^2} = \frac{cos^2 - 1}{m^2 \cdot cos^2} = \frac{-sin^2(\gamma)}{m^2 \cdot cos^2(\gamma)} = -\frac{tg^2(\gamma)}{m^2}.$$

With this in mind, the following formula can be written to determine D:

$$D = \frac{e^{-\frac{tg^2(\gamma)}{m^2}}}{4 \cdot m^2 (\vec{H} \cdot \vec{N})^4}.$$

Let us decompose $e^{-\frac{tg^2(\gamma)}{m^2}}$ in Taylor, limited to two terms $e^{-\frac{tg^2(\gamma)}{m^2}} \approx 1 - \frac{x^2}{m^2}$. Then approximate $e^{-\frac{tg^2(\gamma)}{m^2}}$ by function $cos^{\frac{a}{m^2}}$. In continuation Let us decompose $cos^{\frac{a}{m^2}}$ in Taylor, limited to two terms.

$$cos^{\frac{a}{m^2}} = 1 - \frac{a}{2 \cdot m^2} \cdot x^2.$$

Equating the right parts of the two schedules to the Taylor series, we obtain this equality:

$$1 - \frac{x^2}{m^2} = 1 - \frac{a}{2 \cdot m^2} \cdot x^2.$$

From the last equation, we find that $a = 2$. As follows,

$$e^{-\frac{tg^2(\gamma)}{m^2}} \approx \cos^{\frac{2}{m^2}}(\gamma) .$$

Considering

$$D = \frac{1}{4 \cdot m^2 (\vec{H} \cdot \vec{N})^4} e^{\left(\frac{(\vec{H} \cdot \vec{N})^2 - 1}{m^2 \cdot (\vec{H} \cdot \vec{N})^2}\right)} = \frac{1}{4 \cdot m^2 (\vec{H} \cdot \vec{N})^4} \cos^{\frac{2}{m^2}}(\gamma)..$$

Given that the scalar product of vectors $\vec{H}$ and $\vec{N}$ is $\cos\gamma$, we write the following expression for D

$$D = \frac{1}{4 \cdot m^2 \cdot (\vec{H} \cdot \vec{N})^4} \cos^{\frac{2}{m^2}}(\gamma) = \frac{1}{4 \cdot m^2 \cdot \cos^4(\gamma)} \cos^{\frac{2}{m^2}}(\gamma) = \frac{\cos^{\frac{2}{m^2}-4}(\gamma)}{4 \cdot m^2}.$$

Figure 1 shows a graphic $\frac{\cos^{\frac{2}{m^2}-4}(\gamma)}{4 \cdot m^2}$ and $\frac{e^{-\frac{tg^2(\gamma)}{m^2}}}{4 \cdot m^2 \cos^4\gamma}$. Figure 2 shows a graph of the relative approximation error of function $\frac{e^{-\frac{tg^2(\gamma)}{m^2}}}{4 \cdot m^2 \cos^4\gamma}$ by function $\frac{\cos^{\frac{2}{m^2}-4}(\gamma)}{4 \cdot m^2}$ the angle γ .

The graph shows that the proposed function has a good convergence with the original and that high approximation accuracy is achieved for a significant change interval of the original function.

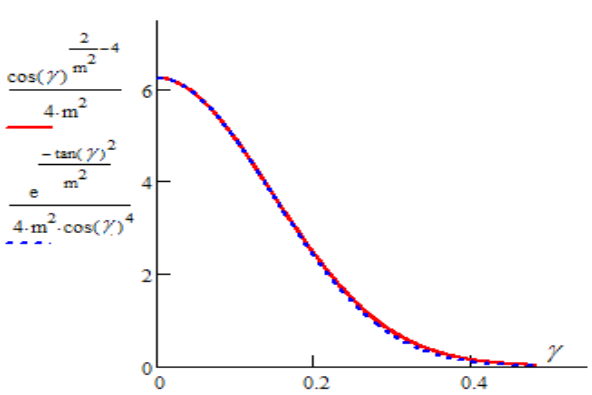

Fig. 1. Graphical comparison of functions

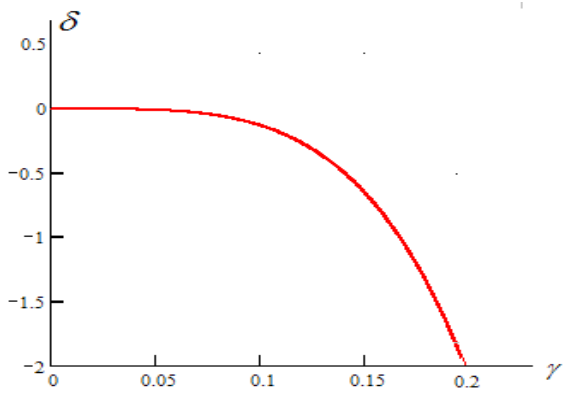

Fig. 2. Relative error dependence on angle γ

The second section shows that [15] $\cos^n\gamma \approx \left(\frac{n}{g}(\cos\gamma - 1) + 1\right)^g$.

Let us use this function to approximate *D*:

$$\frac{\cos^{\frac{2}{m^2}-4}(\gamma)}{4 \cdot m^2} \approx \frac{1}{4 \cdot m^2} \cdot \left(\frac{\frac{2}{m^2} - 4}{g} \cdot (\cos\gamma - 1) + 1\right)^g .$$

After simplification, we get that $\frac{\cos^{\frac{2}{m^2}-4}(\gamma)}{4 \cdot m^2} = \frac{1}{4 \cdot m^2} \left(\cdot(\cos\gamma - 1) + 1\right)^g$

For $g=4$ $D4=\frac{1}{4\cdot m^2}\cdot\left[(\frac{1}{2m^2}-1)\cdot(\cos\gamma-1)+1\right]^4$,

For $g=8$ $D8=\frac{1}{4\cdot m^2}\cdot\left[(\frac{1}{4\cdot m^2}-\frac{1}{2})\cdot(\cos(\gamma)-1)+1\right]^8$,

For $g=16$ $D16=\frac{1}{4\cdot m^2}\cdot\left[(\frac{1}{8\cdot m^2}-\frac{1}{4})\cdot(\cos(\gamma)-1)+1\right]^{16}$.

Fig. 3 shows a graph of the variation in function *D*, *D*4, *D*8 and *D*16. Function *D*16 provided high accuracy of approximation as for the epicenter of the bell-shaped *D*, and for its blooming zone (Fig. 4).

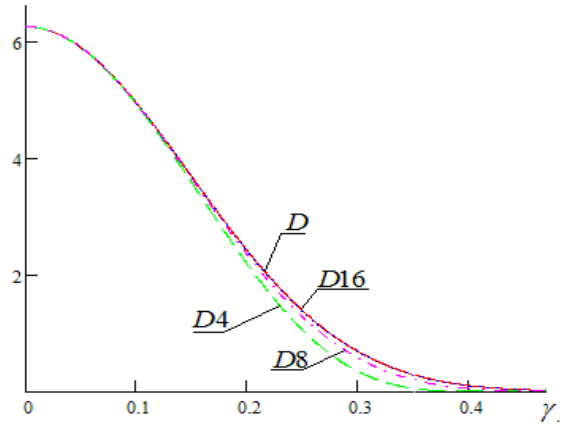

Fig. 3. Graph of variation in function *D*, *D*4, *D*8 and *D*16

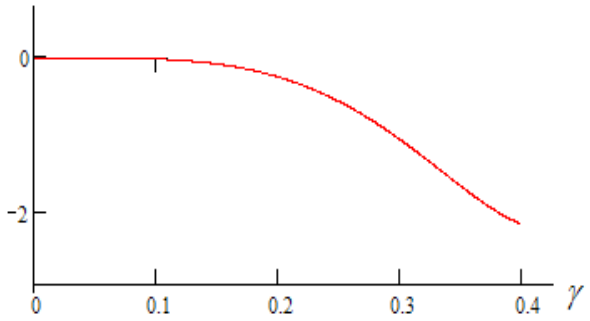

Fig. 4 Relative error of approximation of *D* by *D*16

According to the Ward model, the color intensity is determined by the following formula

$$I_w=\frac{k_d}{\pi}+k_s\cdot\frac{1}{\sqrt{\vec{V}\cdot\vec{N}+\vec{L}\cdot\vec{H}}}\cdot\frac{e^{-\frac{tg^2(\gamma)}{m^2}}}{4\cdot\pi\cdot\alpha^2}.$$

where α is the correction coefficient that depends on the curvature of the surface,

The difference between the Ward model and the Cook-Torrance model is the absence of the Fresnel factor [2,15] and the self-shadowing factor. It is believed that Ward in his model has reached the most accurate fit of this model to the experimental data.

Let us replace $e^{-\frac{tg^2(\gamma)}{m^2}}$ with $\cos^{\frac{2}{m^2}}(\gamma)$. Using these in the second chapter we can rewrite dependence $\cos^n\gamma\approx\left(\frac{n}{g}(\cos\gamma-1)+1\right)^g$ as:

$$I_w\approx\frac{k_d}{\pi}+k_s\cdot\frac{1}{\sqrt{\vec{V}\cdot\vec{N}+\vec{L}\cdot\vec{H}}}\cdot\frac{\cos^{\frac{2}{m^2}}(\gamma)}{4\cdot\pi\cdot\alpha^2}=\frac{k_d}{\pi}+k_s\cdot\frac{1}{\sqrt{\vec{V}\cdot\vec{N}+\vec{L}\cdot\vec{H}}}\cdot\frac{\cos^{\frac{2}{m^2}}(\gamma)}{4\cdot\pi\cdot\alpha^2}=$$
$$=\frac{k_d}{\pi}+k_s\cdot\frac{1}{\sqrt{\vec{V}\cdot\vec{N}+\vec{L}\cdot\vec{H}}}\cdot\frac{\left(\frac{2}{g\cdot m^2}(\cos\gamma-1)+1\right)^g}{4\cdot\pi\cdot\alpha^2}.$$

The analysis showed that a sufficient approximation accuracy is achieved with $g=16$. In this case:

$$I_w = \frac{k_d}{\pi} + k_s \cdot \frac{1}{\sqrt{\vec{V} \cdot \vec{N} + \vec{L} \cdot \vec{H}}} \cdot \frac{\left(\frac{1}{8 \cdot \alpha^2} (\cos\gamma - 1) + 1 \right)^{16}}{4 \cdot \pi \cdot \alpha^2}.$$

The relative error of approximation $e^{-\frac{tg^2(\gamma)}{m^2}}$ does not exceed 1.3%.

The proposed expressions have significantly less computational complexity than the original expressions by using only one function, and to a lesser extent. Figure 5 shows examples of image formation using the developed Cook-Torrence and Ward models.

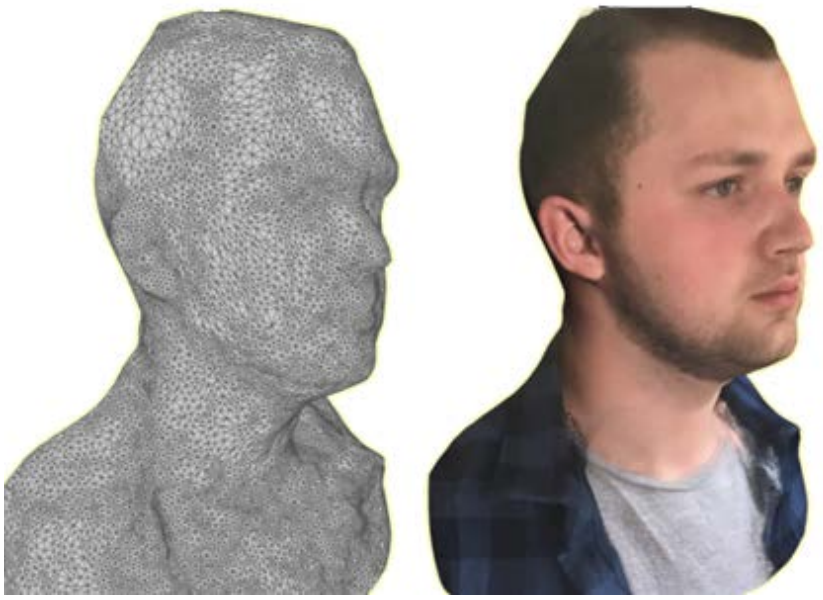

Fig. 5. Examples of face images rendering using the developed modified Ward model

4. RESEARCH RESULTS

A modification of the Cook-Torrance model is proposed by using a new formula to determine the parameter used to calculate the RMS slope of the microfacets. The analysis showed that when using the parameter $D = \frac{1}{4 \cdot m^2} \cdot \left[\left(\frac{1}{8 \cdot m^2} - \frac{1}{4} \right) \cdot (\cos(\gamma) - 1) + 1 \right]^{16}$ instead of $D = \frac{e^{-\frac{tg^2(\gamma)}{m^2}}}{4 \cdot m^2 (\vec{H} \cdot \vec{N})^4}$ allowed to increase the productivity of its calculation by 4.34 times. For the Ward model, productivity gains are more than twice.

5. CONCLUSION

A modification of the Cook-Torrance model is proposed by using a new formula to determine the parameter used to calculate the RMS slope of the microfacets. The analysis showed that when using the parameter $D = \frac{1}{4 \cdot m^2} \cdot \left[\left(\frac{1}{8 \cdot m^2} - \frac{1}{4} \right) \cdot (\cos(\gamma) - 1) + 1 \right]^{16}$ instead of $D = \frac{e^{-\frac{tg^2(\gamma)}{m^2}}}{4 \cdot m^2 (\vec{H} \cdot \vec{N})^4}$ allowed to increase the productivity of its calculation by 4.34 times. For the Ward model, productivity gains are more than twice.

The developed models can be effectively used in systems with highly realistic computer graphics

REFERENCES

[1] Hearn, D.D. and Baker M.P., [Computer Graphics with Open GL], Prentice Hall, 3 edition (2003).

[2] Vyatkin, S., Romanyuk, O., Romanyuk, O.V., Poplavskyy, O. Bazarbayeva, O. and Panas, P., "Modeling the intensity of scattered light and fog using graphics processing units," Proc. SPIE 10808, 108081H (2018).

[3] Romanyuk, O.N. and Chorny, A.V., [High-performance methods and means of painting three-dimensional graphic components: monograph], UNIVERSUM-Vinnytsia, Vinnytsia (2006).

[4] Romanyuk, A., Hast, A. and Lyashenko, Y., "Efficient methods for fast shading," Advances in Electrical and Computer Engineering 8(2), 82–85 (2008).

[5] Vyatkin, S., Romaniuk, O. and Dudnyk, O., "GPU-based rendering for ray casting of multiple geometric data," CEUR Workshop Proceedings 2300, 195–198 (2018).

[6] Vyatkin, S.I., Romanyuk, O.N., Pavlov, S.I., et al., "Offsetting and blending with perturbation functions," Proc. SPIE 10808, 108082Y (2018).

[7] Vyatkin, S.I., Romanyuk, O.N., Pavlov, S.I., et al., "A GPU-based multi-volume rendering for medicine," Proc. SPIE 11045, 1104513 (2019).

[8] Vyatkin, S.I., Romanyuk, O.N., Pavlov, S.I., et al., "Offsetting and blending with perturbation functions," Proc. SPIE 11045, 110450W (2019).

[9] Romaniuk, O., "Approximation of Bidirectional Reflectance Distribution Function with 3-Degree Polynomial," 2007 Siberian Conference on Control and Communications doi**:**10.1109/SIBCON.2007.371317.

[10] Omiotek, Z.,Stepanchenko, O., Wojcik, W., Legiec, W., Szatkowska, M., "The use of the Hellwig's method for feature selection in the detection of myeloma bone destruction based on radiographic images," Biocybernetics and biomedical engineering 39(2), 328-338 (2019).

[11] Kvyetnyy, R., Bunyak, Y., Sofina, O., et al., "Blur recognition using second fundamental form of image surface," Proc. SPIE 9816, 98161A (2015).

[12] Kvyetnyy, R.N., Sofina, O., Orlyk, P., Utreras, A.J., Wójcik, W., et al., "Improving the quality perception of digital images using modified method of the eye aberration correction," Proc. SPIE 10031, 1003113 (2016).

[13] Torrance, K., and Sparrow, E., "Theory for Off-Specular Reflection from Roughened Surfaces," J. Optical Soc. America 57, 1105–1114 (1967).

[14] Ward, G., "Measuring and modeling anisotropic reflection," Proceedings of SIGGRAPH 265–272, doi:10.1145/133994.134078.

[15] Romanyuk, A., Lyashenko, Y., Melnik, A. and Goncharuk, A., "Effective Models for the Specular Color Constituent Computing," Jornal of computer science and engineering 2, 25–29 (2010).